Available online at www.sciencedirect.com
ScienceDirect
Journal of Sound and Vibration 313 (2008) 891–907
JOURNAL OF SOUND AND VIBRATION
www.elsevier.com/locate/jsvi

Coupled head–neck–torso and seat model for car seat optimization under rear-end impact

Nicolas Bourdet*, Rémy Willinger

Strasbourg University, IMFS UMR 7507 ULP CNRS, 2, rue Boussingault F-67000, Strasbourg, France

Received 18 May 2006; received in revised form 27 November 2007; accepted 3 December 2007
Handling Editor: M.P. Cartmell
Available online 31 January 2008

Abstract

The development of new protective systems must be performed on tools reliable and representative of alive human. In an earlier study, a simplified but realistic modelling of the head–neck system under moderate rear impact was performed. In order to address this issue, an original lumped model of the human torso was developed and coupled to a car seat-head rest complex. The experimental modal analysis of the human torso in a seating position performed by Kitazaki in 1992 [Paper presented at the United Kingdom Meeting on Human Response to Vibration held at I.S.V.R. University of Southampton, Southampton, UK, 28–30 September 1992.] was used in the present study for the identification of the mechanical parameters of a lumped human torso model. Despite its low complexity, this model was able to reproduce the five first experimental vibration modes and it was possible to validate it in terms of natural frequencies, damping ratio and mode shapes. In addition to the lumped approach, an external geometry of the human torso was implemented in order to provide a realistic coupling of the human body model to a finite element model of the car seat also developed in the present study. A parametric study was finally carried out in order to evaluate the influence of the torso behaviour and of the different parts of a car seat on the mechanical neck response under rear-end impact. The results of this study allow concluding that the torso behaviour has an important influence on the neck loading and therefore that the quality of a car seat depends on the human body substitute used. For instance, with the proposed torso model, a low-neck injury criterion (NIC) rearward value was obtained with low rigidity of the backrest foam and a stiff backrest net.

1. Introduction

Despite advances in safety devices, neck injuries in traffic accidents, especially non-severe rear impact accidents, are still a serious and costly social problem. The high cost of whiplash injury has been extensively documented in several countries [1,2]. In order to decrease the incidence of whiplash injuries, development of safety measures requires reliability and fidelity of human body surrogates. Most injury prevention strategies are based on impact analysis using anthropomorphic crash test dummies or mathematical models. Improvement of injury prevention techniques needs agreement between both experimental and computational

*Corresponding author. Tel.: +33 3 90 24 29 49; fax: +33 3 88 61 43 00.
E-mail address: bourdet@imfs.u-strasbg.fr (N. Bourdet).

0022-460X/$ - see front matter © 2007 Elsevier Ltd. All rights reserved.
doi:10.1016/j.jsv.2007.12.009

models on the one hand and experimental *in vivo* human body mechanical responses on the other. Unfortunately the spine is one of the most complex structures in the human skeletal system and its behaviour during impact is still poorly understood.

Today no less then three crash test dummies are used in experimental rear impact analysis: The Hybrid III dummy, developed by Foster et al. [3], the BioRID II reported by Davidsson [4] and the RID dummy proposed by Cappon et al. [5]. Several validation studies on neck responses have been carried out on these dummies against volunteers and post-mortem subjects [4–9]. They demonstrated several limitations of this human body surrogate under low speed rear impact in terms of biofidelity. It is unclear if this lack of biofidelity is due to the torso behaviour or the neck characteristics. Optimization studies of the car seat-head rest system described by Svensson et al. [10], Eichberger et al. [11], Ishikawa et al. [12], and Szabo et al. [2] have shown that the safest protective system against whiplash depends on the particular dummy that is being considered. In order to provide realistic boundary conditions to the neck under whiplash loading, the present paper focuses on human torso modelling.

Modelling of the human trunk began in the middle of the last century and existing models can be divided into two categories i.e. continuous models [13] and lumped parameters models [14]. However, most of these models do not have a realistic behaviour compared to the human body. On the one hand, models are often too detailed and involve a high number of parameters that are not easily identified with existing experimental data. On the other hand, they represent only one particular dynamic behaviour of the trunk and can therefore not be used for other applications such as the simulations of rear impacts. Finally, most of the studies concerning the torso aim at characterizing the global dynamic behaviour of the trunk-head system under seat ejection for military applications. In addition, none of them has studied the kinematic behaviour of the first thoracic vertebra (T1) under rear impact, an essential aspect for neck injury investigation.

Several multi-body human models have been developed for rear-end impacts. A two-dimensional human model has been proposed by Jernström et al. [15] and the computed head-torso relative angle was compared to the one recorded on a volunteer undergoing a velocity change of 2.2 m/s. In Jakobsson et al. [16] it was then shown that neither the upper thoracic spine curvature of the model nor the calculated duration of the contact between the head and the headrest were in accordance with experimental data.

As reported, numerical and physical spine models are usually validated against experiments on volunteers or post-mortem human subjects (PMHS) in the time domain by superimposing model and human response parameters as a function of time. This methodology is limited as it is very difficult to characterize a multiple degrees of freedom system under impact in the time domain. The mentioned limitation illustrates the need for further torso experimental and theoretical analysis. The purpose of the present paper is to refer on *in vivo* human trunk characterization available in the literature using modal analysis techniques and to develop a lumped parameters model of this segment in the sagittal plane to be validated in the frequency domain.

In mechanical engineering, modal analysis is a well-known non-destructive technique used for dynamic structures identification. In biomechanics, the method has been extensively used in the field of orthopaedic research and in the dynamic characterization of the human head [17–19]. In previous studies undertaken by Willinger and Bourdet [20], Willinger et al. [20,21] as well as Meyer et al. [22], the experimental *in vivo* modal analysis of the human head–neck system has provided us with natural frequencies and deformed mode shapes of this structure. These results constitute an original validation methodology for dummy necks and will be partly used in the present study. More interestingly, Kitazaki [23] and Kitazaki and Griffin [24] undertook a detailed experimental modal analysis of the whole human column including the head. This study focalized on the analytical transfer functions between input and output, but did not provide any human body mechanical model.

The present study is based on the experimental results reported by Kitazaki [23] as these are used to identify a five original lumped parameters trunk model. In the first section the general methodology is presented including the use of existing experimental modal analysis for the identification of a torso lumped parameter model and its coupling to both the head–neck and the car seat for rear impact applications. In the result section, influence of trunk mobility is analysed through comparison between responses of a rigid and a flexible trunk under a standard rear impact pulse. Finally, a parametric study is performed in order to evaluate the effect of mechanical parameters of the seat on the human neck response.

2. Method

2.1. Experimental modal analysis from the literature

The experimental data used in this study were reported by Kitazaki [23]. The experiment consisted in characterizing the movements of the head and the torso when the body was subjected to vibration. The aim of this research was to determine the natural frequencies, mode shapes and modal damping of the human torso in order to better understand the origin of lumbar pains sustained by truck drivers.

The studied system is shown in Fig. 1 and illustrates the head–neck–trunk unit whose position in the sagittal plan is characterized by 15 degrees of freedom i.e. two head translation (T_x, T_z respectively, antero-posterior horizontal axes and vertical axes) and the head rotation around sagittal axes (θ_y) recorded by an accelerometer amount at head level, and 10 other sensors for the x and z (respectively, horizontal and vertical axes) accelerations of the five vertebrae T1, T6, T11, L3 and S2.

The system was excited by a vibratory platform recording the transmitted force and accelerations. The frequency exciter was able to transmit up to 10 kN with a maximum displacement of 1 m. The vibratory test consisted of a Gaussian random excitation ($\Gamma = 1.7\,\mathrm{m\,s^{-2}}$ (rms), $f = 0$, 5 to 35 Hz; during: 1 min). For a first experimental set, a male subject (1.72 m tall and weighting 65 kg) aged 32 years old and without history of back problems participated in the experiment. Two types of experimental responses were analysed, i.e. the transfer functions in terms of: apparent mass ($A_{jk} = \Gamma_j/F_k$) and in terms of transmissibility: ($T_{jk} = \Gamma_j/\Gamma_k$), where F_k and Γ_k represent the force and the acceleration at platform level, also called inputs.

This representation of the human body allowed the authors to determine the analytical transmissibility equations and to superimpose them with those recorded experimentally. The deformed mode shapes illustrated in Fig. 2, and their quantitative description reported in Table 1 were extracted by this analytical transfer functions. As a whole 11 modes have been identified in this experimental and analytical torso modal analysis between 1.8 and 17 Hz.

While this high quality study can be of great interest in the analysis of car driver comfort, its application in impact biomechanics is limited as it does not provide a mechanical model to be used under loading conditions.

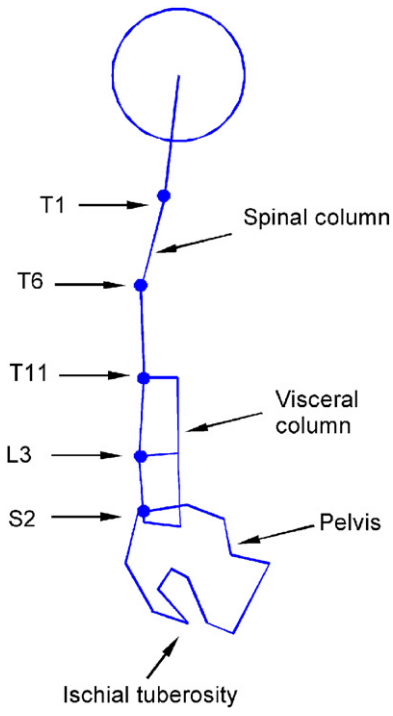

Fig. 1. Degrees of freedom of the human body for modal analysis based on Kitazaki [23] assumption.

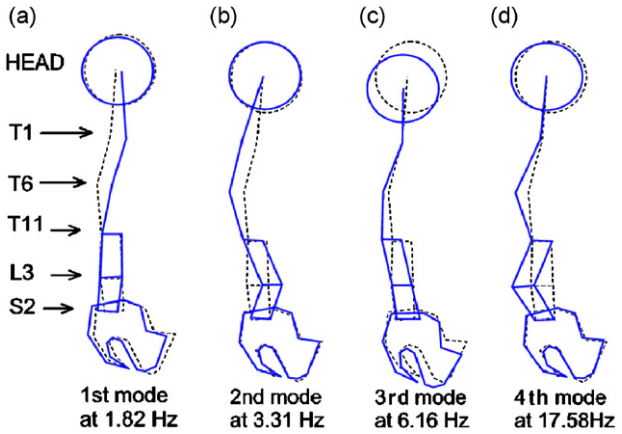

Fig. 2. Representation of the deformed mode shapes extracted by Kitazaki et al. (1998), at 1.82 Hz (a), (b) for 3.31 Hz (b), 6.16 Hz (c), 17.58 Hz (d) (- - - initial position; — vibrated position).

Table 1
Quantitative results of the human body modal analysis

Mode	Natural frequency (Hz)	Damping ratio
1	1.82	0.224
2	3.31	0.215
3	6.16	0.178
4	17.58	0.296

More precisely, the analytical transfer function permits to identify torso natural frequencies and modes shapes, but gives no mechanical parameters such as segment masses or joint rigidity and damping. This issue will be the first step of the torso model development proposed in the present study. A second limitation of Kitazaki's study for the modelling of the human body under rear impact is the poor neck behaviour description linked to the degree of freedom selection at cervical level. This was fortunately addressed in an earlier experimental neck modal analysis published by Willinger et al. in 2003 [25], with results directly integrated in the present study.

2.2. Modelling of the human trunk

In this section, experimental data from Kitazaki [23] were used to establish a minimum complexity lumped parameters model allowing the reproduction of a realistic dynamic behaviour of the human torso. Four relevant deformed mode shapes related to the torso segment are considered for the spinal column modelling. In order to obtain the deformed mode shapes given by Kitazaki [23], the torso model consists of five joints, as illustrated in Fig. 3. In this paper, the hypothesis was made that experiments conducted in an ergonomic environment can be used under crash condition as it focuses on modal characteristics in the frequency domain in order to extract natural frequencies and mode shapes. It is supposed that these modal characteristics can be used under crash condition to describe the initialization of the body motion very early after impact. Due to the small displacements of the trunk against the seat back the trunk behaviour is supposed to be linear so that the dynamical characteristics extracted under modal analysis can be applied for rear impact consideration.

The model consisted of six segments respectively representing the lower and upper lumbar part, the lower and upper thorax, the neck and the head. Mass m_i and inertias J_i from each part are concentrated at their centre of mass G_i. Each joint has a stiffness k_i and a damping ratio c_i. The small angle approximation was adopted. The length of the segments, masses and inertias were determined by anthropometric measurements and calculated using a geometrical model developed by Hanavan [26]. This model represents the human body

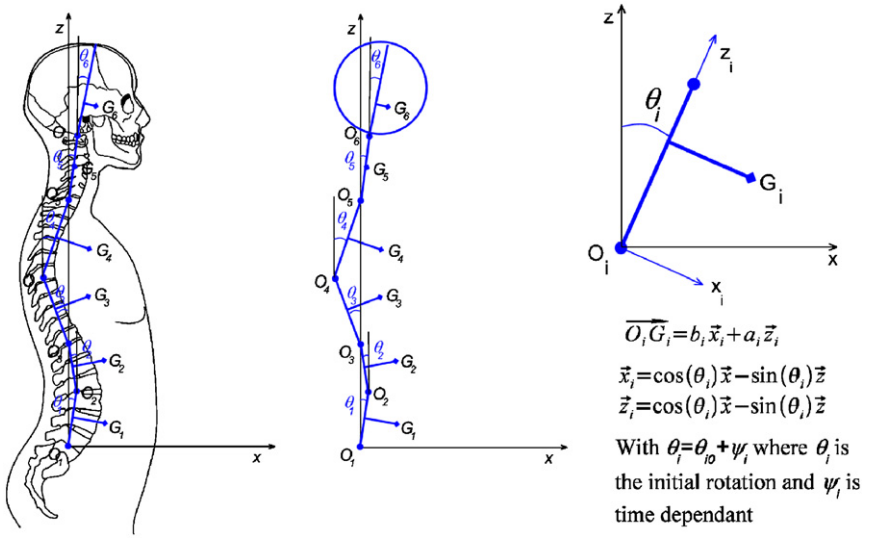

Fig. 3. Illustration of the proposed human trunk lumped parameters model.

Table 2
Mass and inertial data of the trunk, the neck and the head

Parts	Mass (kg)	Inertias/y (kg m^2)
Lower lumbar	3.6	0.01
Upper lumbar	7.3	0.0281
Lower torso	8	0.0352
Upper torso	10.5	0.0603
Neck	1.7	0.002
Head	4.5	0.04

by ellipsoidal and cylindrical segments. The mass components are based on the regression equations reported by Clauser et al. [27]. Finally, masses and inertias are synthesized in Table 2.

The lumped parameters model of the head–neck–trunk unit was implemented into the implicit finite element code ANSYS in order to compute the natural frequencies and the deformed mode shapes of the system.

In order to fit the numerical approach with the experimental configuration provided by Kitazaki [23], vibration displacements were imposed at ischial and pelvis level. Two types of numerical analysis were carried out with this model:

- a free vibration modal analysis, which permitted it to extract the various deformed mode shapes accordingly to the natural frequencies for an elastic behaviour;
- a harmonic analysis in order to identify the exact values of the natural frequencies and the related damping ratios.

The free vibration modal analysis enabled it to determine four deformed mode shapes with natural frequencies over 1 Hz, as illustrated in Fig. 4. These deformed modes shapes can be compared with those obtained by Kitazaki [23] reported in Fig. 2 and there superimposition permitted it to identify stiffness and damping in S2, L3, T11 and T6 joints. As stated earlier neck characteristics i.e. T1 and C0 rigidity were determined in a previous experimental study [20]. Optimization of both parameters stiffness and damping was then carried out with 27 iterations until good accordance of the modal behaviour of the whole model with the experimental data was reached. Tables 3 and 4 report respectively the comparison of the experimental and

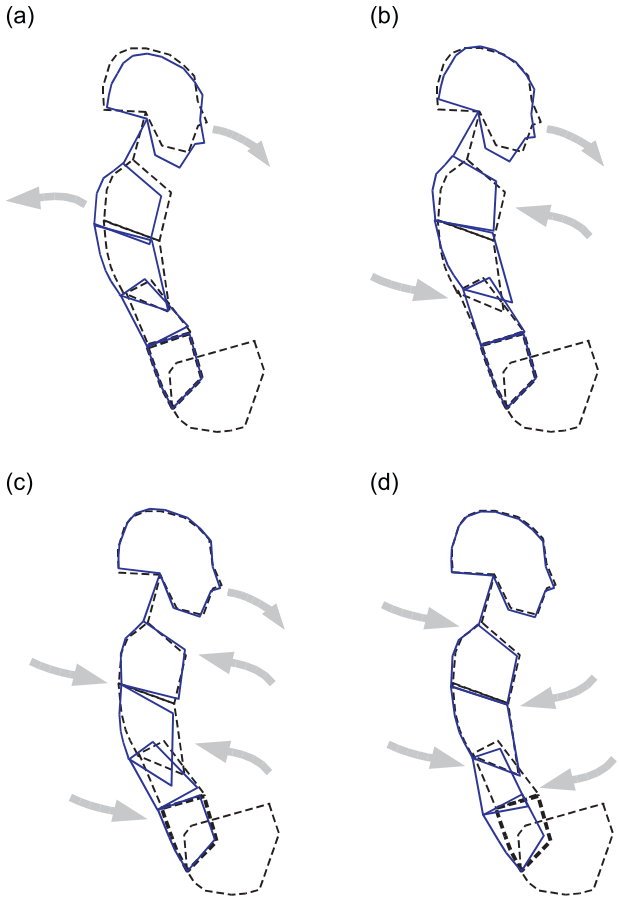

Fig. 4. Representation of four deformed mode shapes obtained under free vibration modal analysis with the proposed lumped model (mode 1 at 1.74 Hz, mode2 at 3.25 Hz, mode 3 at 6.38 Hz and mode 4 at 17.78 Hz).

Table 3
Optimization model behavior compared with the experimental ones reported by Kitazaki et al.

Mode	Natural frequency (Hz)		Damping ratio	
	Exp.	Model	Exp.	Model
Mode 1	1.82	1.90	0.224	0.23
Mode 2	3.31	3.25	0.215	0.21
Mode 3	6.16	6.2	0.178	0.18
Mode 4	17.58	17.2	0.296	0.25

Table 4
Stiffness and damping values of the lumped model

Articulations	k (N m/rad)	c (N m s/rad)
C0	18	0.1
T1	20	0.8
T6	625	0.8
T12	92	0.2
L3	224	0.9
S2	643	0.1

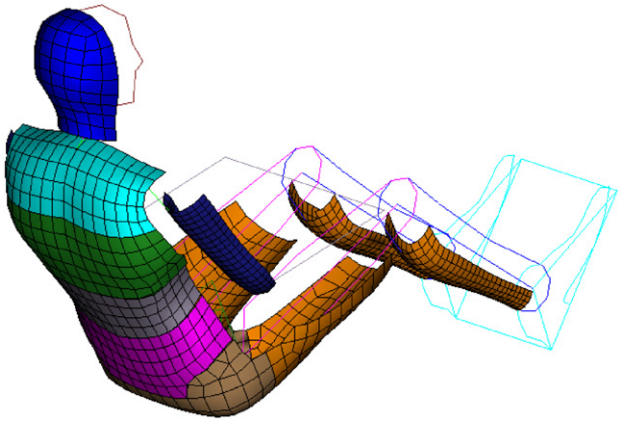

Fig. 5. Integration of the lumped head–neck–torso model into a finite element approach based on realistic contact surfaces.

numerical four first natural frequencies and the torso model mechanical characteristics of the torso model in terms of rigidity and damping.

This lumped model was then implemented into the explicit finite element calculation code used in the crash field as Radioss from MECALOG Corporation in order to couple it with the seat model for rear impact simulation.

In order to reduce the number of elements, the lumped model structure was defined with beam elements. An external shell representing the back of the torso was meshed and fitted to the human lumped model. The geometry of the surface was based on the volunteer's geometry by numerical palpation of his back. This volunteer used only for geometry issues is a 33 years old male close to the 50th percentile (height:1.72 m, weight:72 kg), to whom it was asked to remain seated in a driving position. Each segment is defined as a rigid body in conformity with the lumped model. Masses and inertias, reported in Table 2, are attached to the master node corresponding to the centre of gravity of the considered torso part. Fig. 5 shows that only surfaces in contact with the car seat were meshed such as the upper thorax, the lower thorax, the upper and lower lumbar, the gluteal surface, the thighs, the legs, the arms and the head. These surfaces were essential to carry out the coupling between human body and car seat.

2.3. Car seat modelling

An accurate modelling of the car seat is another essential aspect of rear impact investigation. A car seat consists of various complex mechanical elements. The main parts to be considered are the head-rest clamp, the head-rest foam, the foam or padding of the backrest, the foam of seat base, the backrest spring, and the cover of the seat. In this study, the constitutive laws of the foam and the cover were linear elastic with values extracted from experimental tests. This assumption was supposed acceptable as the study focalizes in non-severe impact.

The modelling of the seat base was very simplified as it has a limited influence in case of rear impact. It therefore consisted of a flexible shell that aimed at limiting the movement of the thighs and pelvis. The mechanical properties of this segment have been extracted from a compression test and lead to a Young's modulus of 1000 MPa and Poisson's ratio of 0.3.

Special attention was paid to the backrest and headrest of the seat. The backrest frame was modelled with shell elements and its geometry was simplified as illustrated in Fig. 6. It was divided into three parts, i.e. the base frame considered as a rigid body, the elastic seat frame, and the upper frame also considered as a rigid body. The seat base and the backrest frame were connected by a spring fixed at the base frame. The sockets maintaining the headrest on the backrest were fixed on the upper frame by a rigid connection.

Whereas the real backrest spring consisted of metal wire connected to the seat frame, the model was composed of three bands represented with shell elements as illustrated in Fig. 7. The sockets were modelled with rigid shell elements and connected to the upper frame by spring elements. In the same manner as for the

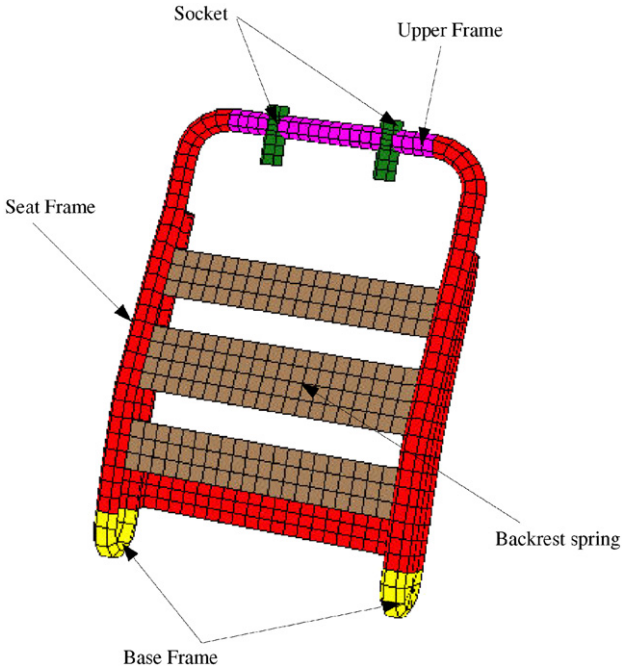

Fig. 6. Details of the car seat backrest frame modelling.

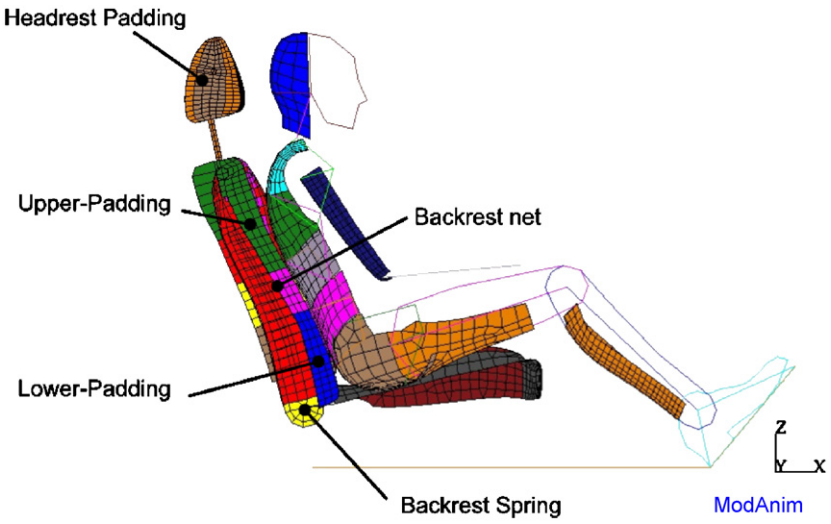

Fig. 7. Positioning of the human model in the seat model and identification of seat parameters for the parametric study.

seat base, the material properties of the backrest spring were determined from a compression test. A Young's modulus of 230 MPa and a Poisson's ratio of 0.29 were obtained. The density was set at 7800 kg/m^3 and the thickness of the bands was 2 mm.

The backrest foam is modelled with 3D brick elements and the foam is divided into the upper parts, the medium part and the lower part. The mechanical properties were determined by compression tests on $100 \times 100 \times 40\,\text{mm}^3$ samples. The material behaviour law used was linear elastic with a Young's modulus of 80 kPa and a Poisson's ratio close to zero. The density of the foam is given by the manufacturer with 40 kg/m^3.

The foam of the seat is covered with a fabric modelled by shell elements whose nodes coincide with those of the external surface. Its mechanical properties have been extracted from static tensile tests and led to a Young's modulus of 1000 MPa.

The headrest model consisted of the clamp and the headrest foam. The clamp is divided into two parts: a deformable part that penetrates into the foam and a rigid part that is fixed to the socket. The 36 kg/m^3 foam is meshed with 3D brick elements with mechanical properties extracted from compression tests leading to a Young modulus of 50 kPa and a Poisson's ratio close to zero. In a similar way as for the backrest, a fabric layer covering the foam was modelled with identical mechanical properties. Finally, the seat base and the backrest frame are bound by a rotational spring with a stiffness of 3300 kN m/rad. If local seat elements were validated with specific tests, a global seat validation test with a dummy was however not performed. The first reason was the objective of the present study which is to couple a simplified seat to an improved human body modelling in order to demonstrate the importance of a realistic torso model in car seat evaluation and the second is that a global seat validation test under impact using an existing dummy would not be efficient as today dummies have quite different behaviour as the present human model.

2.4. Human body-seat coupling under rear impact

In this final step, the human model was coupled with the seat model. In order to have a realistic contact at the beginning of the impact, the trunk curvature was adapted to the seat geometry as illustrated in Fig. 7. The acceleration pulse suggested by EuroNCAP (4.4 m/s) and reported in Fig. 8 was applied to the seat. For this specific rear impact, two human torsos will be considered, the previous development one and a rigid one in order to demonstrate the influence of the human trunk flexibility. For this first analysis a number of parameters will be computed as a function of time in order to evaluate the human body response. Global parameters such as head, upper thorax and pelvis acceleration will be considered but also more neck related outputs as horizontal and vertical acceleration of the first thoracic vertebra (T1), relative displacement and velocity of the first cervical on first thoracic vertebrae (T1-C1), the head–torso relative rotation.

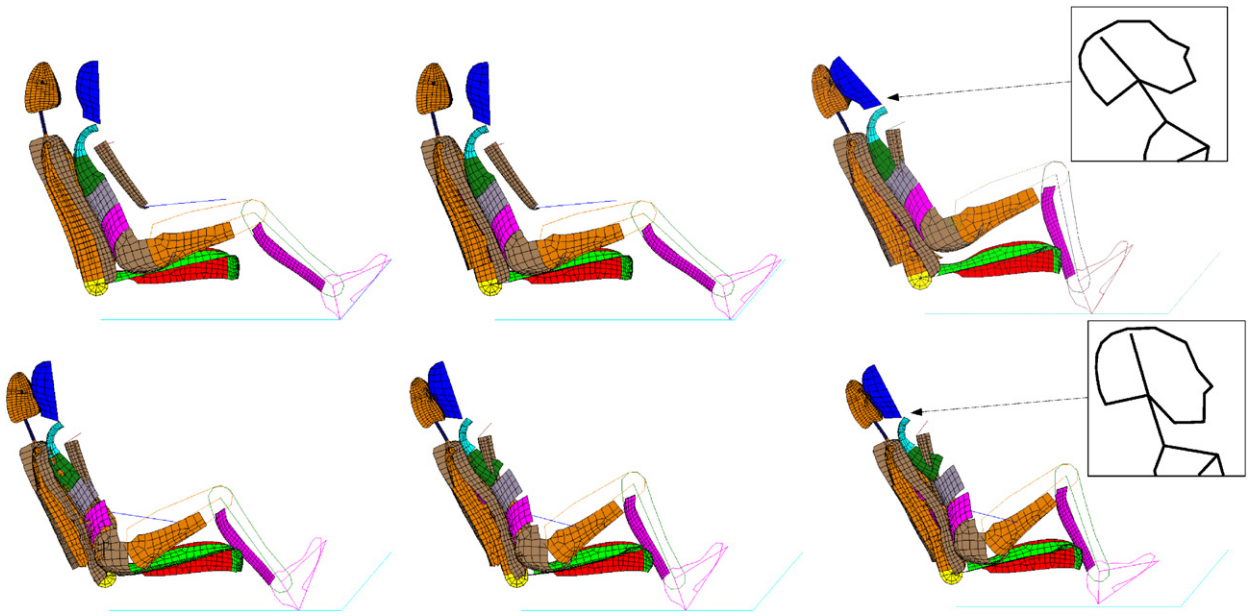

Fig. 8. Illustration of a typical rear end impact simulation with a EuroNCAP pulse at 16 km/h with a rigid torso (top) and flexible torso (bottom) at three time steps (0, 30×10^{-3} and 120×10^{-3} s). It can be observed that the torso behaviour influences drastically the neck response.

Finally, the flexible trunk will be used for a seat parametric study with the objective to identify the relevant seat parameters to be considered in seat optimization. Five seat parameters are considered as illustrated in Fig. 7:

- The upper backrest padding: TOP PAD (elastic law with a Young's modulus of 0.08 or 0.16 MPa);
- The lower backrest padding: BOT PAD (elastic law with a Young's modulus of 0.08 or 0.16 MPa);
- The headrest padding: HR PAD (elastic law with a Young's modulus of 0.05 or 0.5 MPa);
- The backrest net: BCK NET (elastic law, Young's modulus of 230 or 460 MPa);
- The backrest spring: BCK STIFF (between the downseat and the backrest) 17 or 22.5 kN/m.

These five parameters conducted to 16 virtual seats. However, a fractional plan [28] with eight simulations made it possible to perform this analysis. The eight virtual seats coupled to the new human body model are then subjected to the previous defined standard rear impact pulse and following neck injury criteria are computed:

- the bending neck moment at occipital condyle (My),
- the shear force at C1 level in antero-posterior direction,
- the axial force at C1 level in vertical direction,
- head–neck and neck–torso relative angular velocity, and
- the NIC rearward value [29] is an injury criterion for whiplash defined by Eq. (1).

$$\mathrm{NIC}(t) = 0.2a_{\mathrm{rel}}(t) + v_{\mathrm{rel}}^2(t), \tag{1}$$

where

$$a_{\mathrm{rel}}(t) = a_x^{T1}(t) - a_x^{\mathrm{Head}}(t) \quad \text{and} \quad v_{\mathrm{rel}}(t) = \int a_{\mathrm{rel}}(t)\,\mathrm{d}t,$$

$a_x^{T1}(t)$ is the acceleration–time curve measured in the antero-posterior (x) direction at the location of the first thoracic vertebra and $a_x^{\mathrm{Head}}(t)$ the acceleration–time curve measured in the antero-posterior (x) direction at the location of the centre of mass of the head.

3. Results

3.1. Influence of torso flexibility

The results of the simulations are considering successively the new torso model and a rigid torso model as illustrated by the selected pictures in Fig. 8.

The view cached 120 ms after impact, show important differences in dynamic behaviour of the torso and head–neck systems. This can be illustrated by an important rise of the body and a significant head extension in the case of a rigid trunk, whereas a flexible trunk leads to a torso extension with a marked neck retraction motion as illustrated in Fig. 8. Fig. 9a shows the superimposition of the x-accelerations at T1 level, for both torso models and reveals significant difference in slope (62.5%) and in amplitude (34.5%). T1-x displacement is much more significant when the thorax is rigid, as illustrated in Fig. 9b. This is due to the fact that the backrest is loaded by the entire trunk mass in the case of a rigid trunk, while the mass borne by the backrest is much lower with a flexible thorax. This phenomenon is also described in Fig. 9c for T1-z displacement. Such a difference in T1 loading implies a radically different dynamic behaviour of the head and neck system, as shown in Fig. 9d, e and f for respectively C1-T1 relative displacement, head-torso relative rotation and C1-T1 relative velocity parameters, which are supposed to be linked to whiplash induced injury mechanisms. A different kinematic at T1 level causes a more significant C1-T1 relative displacement for a rigid trunk (93 mm) than for a flexible one (77 mm), as illustrated in Fig. 9d. The C1-T1 relative velocity curves also shows important differences, as illustrated in Fig. 9f. As for the head-torso relative rotation curves shown in Fig. 9e, a positive values of this angle illustrates a retraction movement that

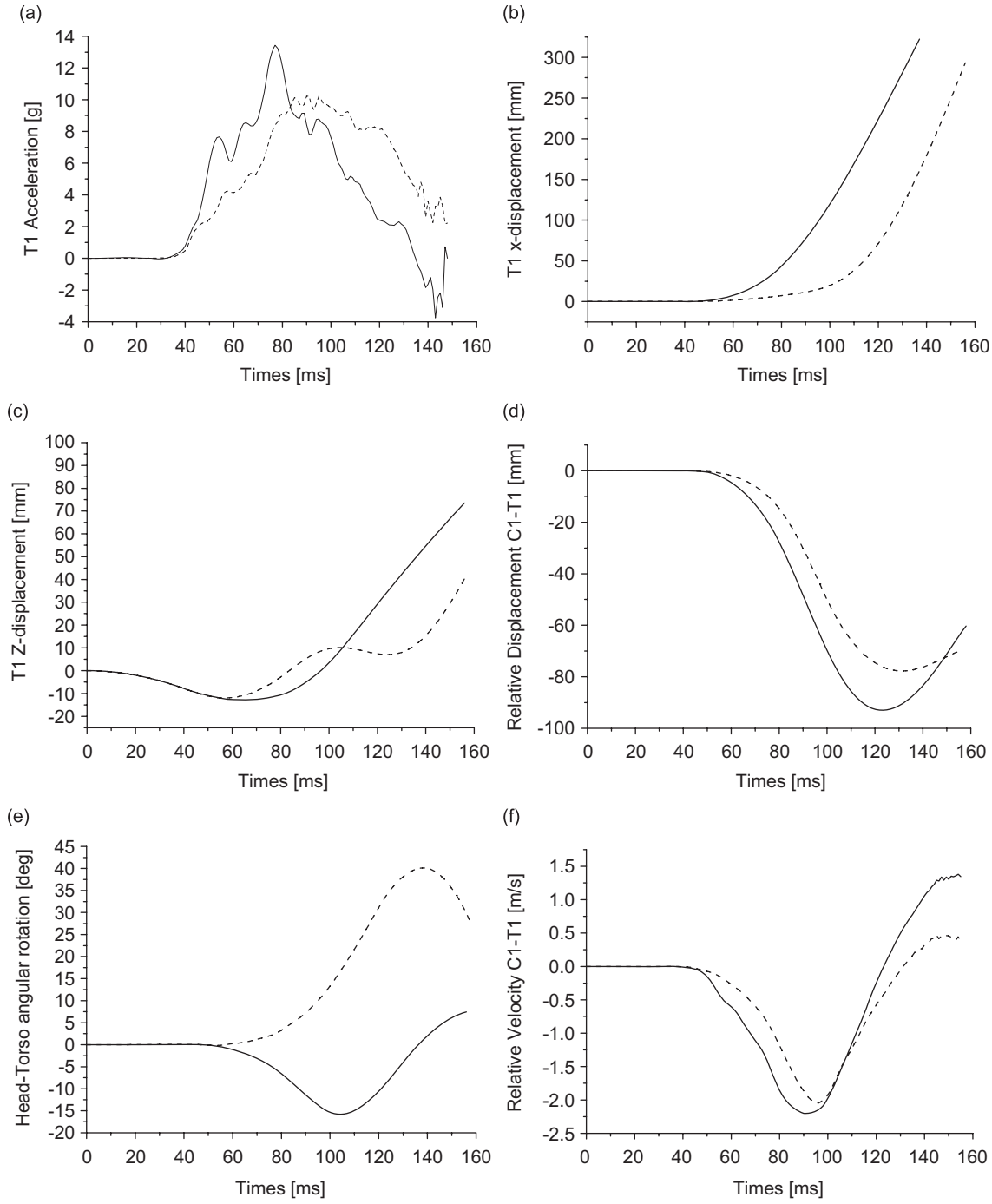

Fig. 9. Superimposition of computed results in terms of (a) T1-x acceleration, (b) T1-x displacement, (c) T1-z displacement, (d) relative C1-T1displacement, (e) Head–torso rotation and (f) relative C1-T1 velocity for both rigid and flexible human trunk model under rear impact (— rigid human trunk; - - - flexible human trunk).

can be observed on the flexible trunk. On the contrary, for the rigid trunk, the head-torso relative rotation negative (extension movement) early after impact and then positive (retraction movement caused by the headrest).

3.2. Seat parametric study

With a final objective that is the seat optimization, a parametric study on main mechanical properties, according to Table 5, was carried out in order to evaluate their influence on the human body.

Table 5
Configuration of the different simulations

No. sim.	TOP-PAD	BOT-PAD	HR-PAD	BCK-NET	BCK-STIFF
1	−	−	−	−	+
2	+	−	−	+	−
3	−	+	−	+	−
4	+	+	−	−	+
5	−	−	+	+	+
6	+	−	+	−	−
7	−	+	+	−	−
8	+	+	+	+	+

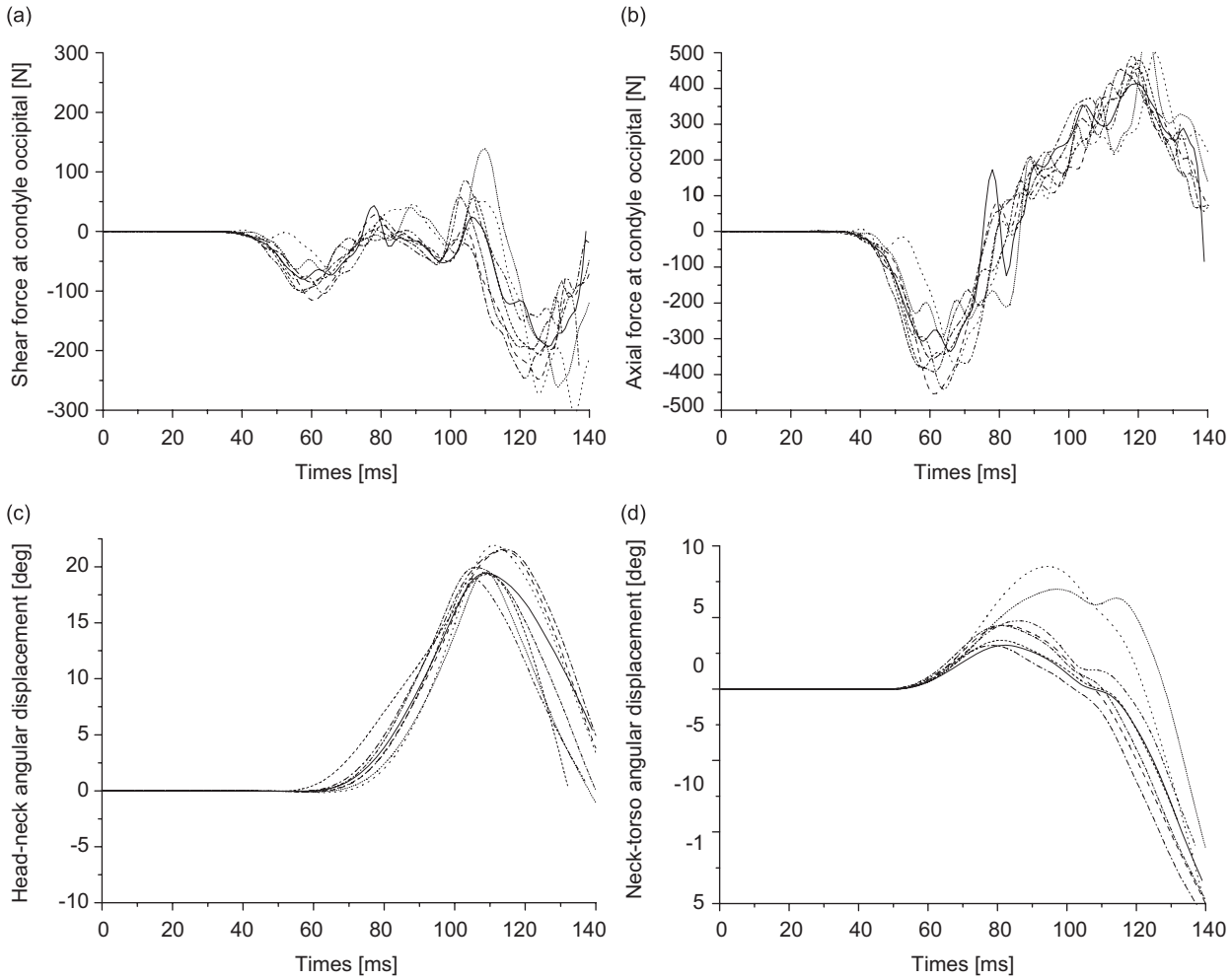

Fig. 10. Results of the eight simulations in terms of (a) shear force at occipital condyle, (b) axial force at occipital condyle, (c) relative head–neck rotation and (d) relative neck–torso rotation (— simulation 1; –– simulation 2; - - - simulation 3; - · - simulation 4; - · · simulation 5; - - - simulation 6; · · · · · simulation 7; - · - · simulation 8).

Table 6
Different values used for the parametric study

	TOP-PAD (Mpa)	BOT-PAD (Mpa)	HR-PAD (Mpa)	BCK-NET (Mpa)	BCK-STIFF (kN)
–	0.08	0.08	0.05	230	17
+	0.16	0.16	0.5	460	22.5

Table 7
Tendencies of factors for a seat optimization (↓ low rigidity, ↑ high rigidity, → no influent)

	Fx	Fz	My	$\Delta\dot{\theta}_{HN}$	$\Delta\dot{\theta}_{NT}$	NIC
TOP-PAD	↓	↑	→	↑	↑	↓
BOT-PAD	↓	↓	↓	↓	↓	↓
HR-PAD	→	↓	→	→	→	→
BCK-NET	↓	→	→	↓	↓	↑
BCK-STIFF	→	↑	↑	↑	↑	→

Results in terms of neck loading (shear and axial force) as well as kinematics (relative rotation) and injury criteria (NIC) were computed for each seat and superimposed in Fig. 10a–d. A detailed comparative analysis of these results is reported hereafter and synthesized in Tables 6 and 7.

3.2.1. *Neck axial and shear force at occipital condyle*

Neck loading in terms of force is often considered to be an injury parameter. The lower backrest padding (BOT-PAD) is the most important factor influencing the shear forces at occipital condyle level, as shown in Fig. 11a. Indeed, an increase of stiffness generates an increase of the shear force at upper neck level. The tensile force is essentially influenced by the backrest spring, as an increase of this parameter reduces it drastically (Fig. 11b).

3.2.2. *Neck moment at occipital condyle*

The moment at the occipital condyle is another essential parameter and strongly depends on the rigidity of the lower backrest padding, as illustrated by Fig. 11c. This figure shows that an increase of this rigidity tends to increase the moment. The backrest spring is also a significant factor tending to reduce the moment by its increase as for the axial force.

3.2.3. *Head–neck and neck–torso relative angular velocity*

The three most influential factors, after the backrest spring, for the relative angular velocity are the upper and lower backrest padding as well as the backrest net. Fig. 11d and e show that the harder the foam of the upper backrest is, the lower are the head–neck and neck–torso relative angular velocities.

3.2.4. *NIC criteria*

NIC is becoming more and more a standard in experimental seat evaluation. By studying the various parameters, one can observe that several contradictions appear. The different parts of the seat that influence the most the NIC value are the backrest net and the upper backrest padding as observed in Fig. 11f. Indeed, contrary to the upper backrest padding, an increase of the backrest net rigidity decreases the NIC. These contradictions do not allow to optimize the seat easily under rear-end impact.

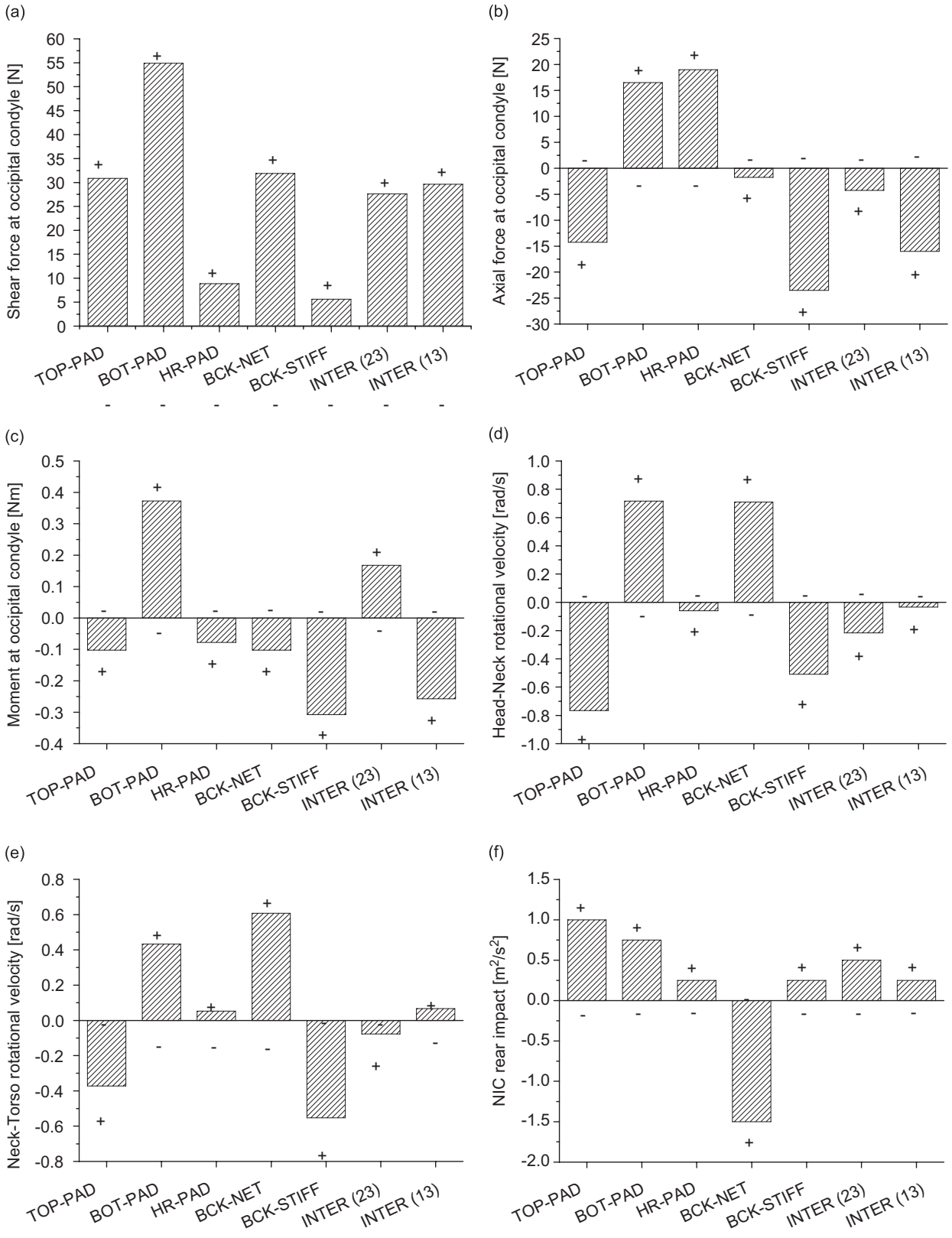

Fig. 11. Representation of the influence of each seat factor in terms of (a) shear force, (b) axial force at occipital condyle, (c) moment at occipital condyle, (d) head–neck rotational velocity, (e) neck–torso rotational velocity and (f) NIC rear impact ($\pm$ sign indicates the minimum and maximum value of the related seat mechanical parameter [28]).

Table 8
The assumed best seat

Part of the seat	Best seat
TOP-PAD	0.16 MPa
BOT-PAD	0.08 MPa
HR-PAD	0.275 MPa
BCK-NET	230 MPa
BCK-STIFF	22.5 kN

4. Discussion

The discussion of this new human body-seat model is divided into two parts. The first one is about the validation of the human trunk model itself, and the second deals with the results relative to a tentative seat optimization study.

Most of the studies related to spine characterization were conducted in terms of intervertebral loading and kinematics in the time domain [30,31]. Kitazaki [23] have applied modal analysis technique and extracted deformed modes which four of them correspond to the spinal column deformations. The analysis was carried out in a comfort issue, and the modelling was restricted to the analytical transfer function rather than to the mechanical characterization of the human body that is necessary for an impact issue. The linearity of the system was checked with the coherence function which remained close to 1. The superimposition of the numerical modal analysis with the experimental results made it possible to define the stiffness and damping parameters for each joints of an original lumped trunk model. Even if a more realistic modelling of the human torso behaviour is proposed in the present study, it must be mentioned that the model validation is limited to the sagittal plane and based on one single 32 years old human male volunteer. Further analysis including female is therefore needed. Nevertheless for a low energy rear end impact, the deformation of the torso remains small, so modal analysis can well reproduce the initialization of the movement.

A number of validation and comparative studies of rear impact dummies are reported in the literature [5,9,32]. All of them were carried out in the time domain showing mechanical parameters versus time. The main improvement observed in recent rear impact dummies was a more flexible spine than for Hybrid III dummy [33,34]. Two comparative studies [7] demonstrated that BioRID and RID2 had very similar responses under moderate impact although BioRID had a flexible thorax. This experimental result is in total disagreement with the present study. Moreover Prasad et al. [7] concluded that Hybrid III is suitable for rear impact testing in the 8–24 km/h range when Philippens et al. [35] had the opposite point of view. All these contradictions can be explained by a not enough accurate human body surrogate response under impact. In fact, the dummies are validated against volunteer and cadaver kinematics including a large scattering in the time domain. This kind of validation, based on quite large response corridors, is not accurate enough to extract the complex dynamic behaviour of the torso. Other contradictions appeared in the time domain when Philippens et al. [35] found an acceptable dummies head kinematics for rear impact whereas T1 kinematics was not. One might wonder how the head can have a biofidelic behaviour while T1 does not, given that T1 is the input of the head–neck loading. In addition to the difficulty related to the time domain analysis, authors such as Kim et al. [32] and Szabo et al. [1], often add complexity by considering seat and thorax effect for dummy neck validation. In the present study, it has been shown that a flexible thorax gave clearly different T1 responses compared to a rigid thorax. Therefore, realistic boundary conditions applied to the head–neck system changes drastically the kinematics and the loading of the head–neck system.

Concerning the seat parametric study, the main limit lies in the modelling of the mechanical properties of the different parts of the seats. Indeed, to redefine the material properties with adapted laws would bring a more complete approach of this pilot optimization study. However, the reported results make it possible to illustrate the predominant influence of the backrest and headrest rigidity. As the ''best'' seat depends on the biomechanical criteria, the average influence for each part of the seat was extracted using an original human body model validated in the frequency domain. Accordingly to the approach designed in this study, an optimal seat would be the one defined in Table 8. As a number of neck injury criteria is proposed in the

literature, a seat optimization minimizing all criteria seems not to be easy. If this shows that further seat modelling should be performed, it also demonstrates that it is essential to improve biomechanical understanding of neck injury mechanisms, an aspect which was not the purpose of the present study.

5. Conclusion

Based on the experimental modal analysis of the human trunk provided by Kitazaki [23], it was possible in the present study to define a lumped mechanical model of the human trunk with five degrees of freedom. The proposed model distinguishes four masses, representing the upper thorax, the lower thorax, the upper lumbar and the lower lumbar, connected with dumped spring joints identified through the experimental data. This original model was able to reproduce the natural frequencies and deformed mode shapes of the torso extracted by the previous authors, a modal superimposition which validated the model. Coupled with a car seat model also developed in the present study and a head–neck model reported in an earlier paper the complete head–neck–torso–seat complex was used to simulate rear end impact more realistically than existing models or crash dummies do.

A comparative study based on a rear impact simulation with a rigid and a flexible human torso, revelled the drastic influence of the trunk flexibility. The boundary conditions of the head–neck unit, imposed by the first thoracic vertebrae kinematics, showed a very different dynamic response of the head and neck when a flexible torso was considered. This dynamic behaviour difference can be illustrated by an important rise of the body and an amplified head extension in the case of a rigid trunk whereas a flexible trunk shows a torso extension with a marked neck retraction movement. It then becomes essential to consider a realistic modelling of the dynamic behaviour of the torso to improve the protection capability of seat under low speed rear end impact. A parametric study of the seat focalizing on five seat parameters allowed it to investigate the influence of the seat on the neck loading and kinematics. Main results show that backrest padding is the most important factor for the shear force and the moment at occipital condyle as an increase of this parameter also increase the neck loading. The relative head–neck and neck–torso angular velocity are influenced by the backrest net as well as the backrest padding, but not in the same way. Indeed, an increasing of the backrest net and the lower backrest padding rigidity increased the relative angular velocity, whereas these parameters decreased with the upper backrest padding rigidity. Lastly, the results give a NIC which decreases when the rigidity of the upper backrest foam decreases and the rigidity of the backrest net increases. A main conclusion of this parametric study is that as long as a large number of neck injury criteria is considered a seat optimization minimizing all criteria is not possible. This indicates that a better understanding of neck injury mechanisms is needed.

In a future development this improved human body lumped model can be coupled to a detailed neck FEM model in order to compute the cervical column and ligament system response under accidental conditions. Only when realistic neck injury criteria will be fixed, the final objective of seat optimization against biomechanical criteria can be achieved.

References

[1] T.J. Szabo, J.B. Welcher, Human Subject kinematics and electromyographic activity during low speed rear impacts, *Proceedings of the 40th Stapp Car Crash Conference*, Vol. 1, SAE 962432, Albuquerque (USA), 1996, pp. 339–356.

[2] T.J. Szabo, D.P. Voss, J.B. Welcher, Influence of seat foam and geometrical properties on BioRID P3 kinematic response to rear impacts, *Proceedings of the IRCOBI Conference*, Vol. 1, Munich (Germany), 2002, pp. 87–101.

[3] J.K. Foster, J.O. Kortge, M.J. Wolanin, Hybrid III—a biomechanically-based crash test dummy, *Proceedings of the 21st Stapp Car Crash Conference*, Vol. 1, SAE 770938, New York, USA, 1977, pp. 975–1014.

[4] J. Davidsson, *BioRID II Final Report*, Crash Safety Division, Department of Machine and Vehicle Design, Chalmers University of Technology, Göteborg, Sweden, 1999.

[5] H. Cappon, M. Philippens, v. Ratingen, J. Wismans, Development and evaluation of a new rear-impact crash dummy: the RID2, *Proceedings of the 45th Stapp Car Crash Conference*, Vol. 1, SAE 2001-22-0010, San Antonio, USA, 2001, pp. 225–238.

[6] M.R. Seemann, W.H. Muzzy, L.S. Lustick, Comparison of human and Hybrid III head and neck response, *Proceedings of the 30th Stapp Car Crash Conference*, Vol. 1, SAE 861892, USA, 1986, pp. 291–312.

[7] P. Prasad, A. Kim, D.P.V. Weerappuli, Biofidelity of anthropomorphic test devices for rear impact, *Proceedings of the 41th Stapp Car Crash Conference*, Vol. 1, SAE 973342, USA, 1997, pp. 387–415.

[8] J. Davidsson, P. Lövsund, K. Ono, M. Svensson, S. Inami, A comparison between volunteer, BioRID P3 and Hybrid III performance in rear impact, *Proceedings of the IRCOBI Conference*, Sitges (Spain), Vol. 1, 1999, pp. 165–190.
[9] G.P. Siegmund, B.E. Heinrichs, J.M. Lawrence, M. Philippens, Kinetic and kinematic responses of the RID2a, hybrid III and human volunteers in low-speed rear-end collisions, *Proceedings of the 45th Stapp Car Crash Conference*, Vol. 1, SAE 2001-22-0011, San Antonio, USA, 2001, pp. 239–256.
[10] M. Svensson, P. Lövsund, Y. Håland, S. Larsson, The influence of seat-back and head-restraint properties on the head–neck motion during rear-impact, *Proceedings of the IRCOBI Conference*, Vol. 1, Eindhoven, The Netherlands, 1993, pp. 395–406.
[11] A. Eichberger, B. Geigl, A. Moser, B. Fachbach, H. Steffan, W. Hell, K. Langwieder, Comparison of different car seats regarding head–neck kinematics of volunteers during rear end impact, *Proceedings of the IRCOBI Conference*, Vol. 1, Dublin, Ireland, 1996, pp. 153–164.
[12] T. Ishikawa, N. Okano, K. Ishikura, An evaluation of prototype seat using Biorid-P3 and Hybrid III with TRID neck, *Proceedings of the IRCOBI Conference*, Vol. 1, Montpellier, France, 2000, pp. 379–391.
[13] J.L. Hess, C.F. Lombard, Theoretical investigations of dynamic response of man to high vertical acceleration, *Aviation Medicine* 29 (1958).
[14] A.P. Vulcan, A.I. King, G.S. Nakamura, Effects of bending on the vertebral column during +Gz acceleration, *Aerospace Medicine* 41 (1970) 294.
[15] C. Jernström, G. Nilsson, M.Y. Svensson, A first approach to an implementation in MADYMO of a human body model for rear impact modeling, *Proceedings of the Fourth International Madymo User's Meeting*, September 6–7, Eindhoven, The Netherlands, 1993.
[16] L. Jakobsson, H. Norin, C. Jernström, S.-E. Svensson, P. Johnsén, I. Isaksson-Hellman, M.Y. Svensson, Analysis of different head and neck responses in rear-end car collisions using a new humanlike mathematical model, *Proceedings of the IRCOBI Conference*, Lyon, France, 1994, pp. 109–126.
[17] V.R. Hodgson, E.S. Gurdjian, L.M. Thomas, The determination of response characteristics of the head when impacting another body, with emphasis on mechanical impedance techniques, *Proceedings of the 11st Stapp Car Crash Conference*, Vol. 1, SAE 670911, 1967, pp. 125–138.
[18] R.L. Stalnaker, J.L. Fagel, Driving point impedance characteristics of the head, *Journal of Biomechanics* 4 (1971) 127–139.
[19] R. Willinger, D. Cesari, Evidence of cerebral movement at impact through mechanical impedance methods, *Proceedings of the IRCOBI Conference*, Bron, France, 1990.
[20] R. Willinger, N. Bourdet, R. Fischer, F. Le Gall, Modal analysis of the human neck *in vivo* as a criterion for crash test dummy evaluation, *Journal of Sound and Vibration* 287 (3) (2005) 405–431.
[21] R. Willinger, N. Bourdet, F. Le Gall, Characterization and modeling of the human head–neck in the frequency domain, *Proceedings of the Fifth International Conference on Vibration Engineering*, Nanjing, 2002, pp. 167–173.
[22] F. Meyer, N. Bourdet, C. Deck, R. Willinger, J.S. Raul, Human neck finite element model development and validation against original experimental data, *Stapp Car Crash Journal* 48 (2004) 177–206 (SAE 2004-22-0008).
[23] S. Kitazaki, Application of experimental modal analysis to the human whole-bodyvibration, *Proceedings of the United Kingdom Informal Group Meeting on Human Response to Vibration*, The University of Southampton, Southampton, Hampshire, 1992, pp. 17–39.
[24] S. Kitazaki, M.J. Griffin, Resonance behaviour of the seated human body and effects of posture, *Journal of Biomechanics* 31 (1998) 143–149.
[25] R. Willinger, N. Bourdet, R. Fischer, F. Le Gall, New method for biofidelity evaluation of dummy necks, *18th ESV Conference*, 18ESV-000343, Nagoya, Japan, 2003.
[26] E.P. Hanavan, A mathematical model of the human body, Paper presented at AMRL-TR-64-102, AD-608-463. Aerospace Medical Research Laboratories in Wright-Patterson Air Force Base, OH, USA, 1964.
[27] C.E. Clauser, J.T. McConville, J.W. Young, *Weight, Volume and Center of Mass of Segments of the Human Body*, Wright Patterson Air Force Base, OH, USA, 1969.
[28] J. Goupy, Introduction aux plans d'expériences, Dunod 2ème Ed., Paris, France, 2001.
[29] Boström Ola, Häland Yngve, Fredikssson Rikard, Autoliv Research Sweden, Svensson Y. Mats, Mellander Hugo, Chalmers University of Technology Sweden, 16th ESV Conference, Windsor, Canada, 1998.
[30] H. Mertz, L. Patrick, Strength and response of the human neck, In: S. Backaitis (Ed.), Biomechanics of Impact Injury and Injury Tolerances of the Headneck Complex, 1993, pp. 821–846; SAE 710855, 1971.
[31] M. Panjabi, J. Wang, N. Delson, Neck injury criterion based on intervertebral motions and its evaluation using an instrumented neck dummy, *Proceedings of the IRCOBI Conference*, Sitges, Spain, 1999, pp. 179–190.
[32] A. Kim, K.F. Anderson, J. Berliner, C. Bryzik, J. Hassan, J. Jensen, M. Kendall, H.J. Mertz, T. Morrow, A. Rao, J.A. Wozniak, A comparison of the Hybrid III and BioRID II dummies in low-severity, rear-impact sled tests, *Proceedings of the 45th Stapp Car Crash Conference*, Vol. 1, San Antonio USA, SAE 2001-22-0012, 2001, pp. 375–402.
[33] J. Davidsson, M.Y. Svensson, A. Flogård, Y. Håland, L. Jakobsson, A. Linder, P. Lövsund, Wiklund. BioRID I—A New Biofidelic Rear Impact Dummy, *Proceedings of the IRCOBI Conference*, 1998, pp. 377–390.
[34] J. Thunnissen, M. van Ratingen, M. Beusenberg, E. Janssen, A dummy neck for low severity rear impacts, *Proceedings of the ESV Conference* 1996, Paper 96-S10-O-12, 1996.
[35] M. Philippens, H. Cappon, M. van Ratingen, J. Wismans, M. Svensson, F. Sirey, K. Ono, N. Nishimoto, F. Matsuoka, Comparison of the rear impact biofidelity of BioRID II and RID2, *Proceedings of the 46th Stapp Car Crash Conference*, Vol. 1, SAE 2002-22-0023, 2002, pp. 383–399.